JOURNAL OF MATERIALS SCIENCE 10 (1975) 1751–1762

Tensile creep and deformation mechanisms in oriented low-density polyethylene

A. COWKING
School of Physics, Robert Gordon's Institute of Technology, Aberdeen, UK

Low density polyethylene (LDPE) which had been uniaxially oriented by cold drawing was stressed parallel to the fibre axis at 20° C. In most of the experiments static tensile loads were applied. Changes in the internal texture and molecular orientation during tensile deformation and recovery were determined by low- and wide-angle X-ray diffraction. Instantaneous elasticity, both in tension and recovery, occurred by extension of the macrolattice formed of layered crystalline and amorphous regions, of which the volume of the material was found to be mainly comprised. Tensile creep was observed having a retardation time for the main process of about 70 h, and was not produced by simple changes in the geometry of the macrolattice. Relaxation mechanisms which could account for slow viscoelasticity in this fibrous material are discussed, and the results are analysed with reference to earlier work on these subjects.

1. Introduction

Oriented crystalline polymers are widely used in load-bearing applications and there has been much study of their structure and deformation under axial load. Deformation mechanisms are not well understood, however. In fibres and drawn films the macromolecules are mainly oriented parallel to the drawing axis: in polyethylene the aligned chain axes are the *c*-axes of the orthorhombic unit cell of the crystalline component, while the *a*- and *b*-axes are usually distributed randomly in the plane normal to the fibre direction. A principal feature of the fibre texture in crystalline high polymers is that along the fibre axis there usually exists a periodicity of magnitude some hundreds of Angstroms which is established to be a fairly regular alternation of partially chain-folded crystals and intervening amorphous layers. The heterogeneity of electron density which results from this fibre long period accounts for the discrete meridional maxima in the X-ray pattern at small angles when the X-ray beam is directed perpendicular to the fibre axis. In addition to the long period structure it has been widely propounded (see, for example, [1–3]) that the stacked crystals are incorporated into fibrils which are long, narrow units having high axial strength, a high ratio of surface to cross-sectional area, and are aligned parallel to the orientation axis. Bundles of fibrils are held together by interfibrillar tie-molecules and Van der Waals forces. Further, there is much evidence of planar crystalline lamallae in some polymer fibres. It has been pointed out [3] that the presence of fibrils does not preclude the existence of lamellae, since there can be lateral register between crystal blocks in adjacent fibrils. The main features of the polymer fibre as outlined above are shown schematically in Fig. 1.

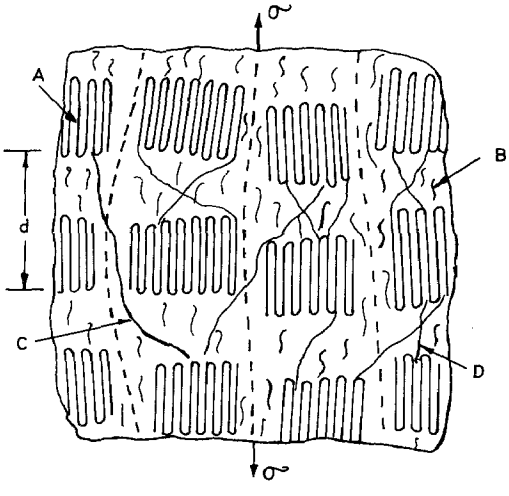

Figure 1 Structural scheme of an oriented crystalline polymer. A: chain-folded crystal, B: amorphous polymer, C: interfibrillar tie-molecule, D: interfibrillar tie-molecule, d: fibre long period.

It has been observed [4–8] in deformations of various oriented polymers at room temperature produced by stresses parallel to the orientation axis that the long period in all cases grows when the polymer is under tensile stress and decreases when under compressive stress. However, in some of these earlier results, e.g. for various linear polymers in tension [6, 7], the relative change in the long period resolved along the stress axis was found to be similar to the macroscopic strain of the fibre along its axis, while in other cases, notably for LDPE in tension [7, 8], this direct correspondence did not hold. There is thus an apparent anomaly that in some cases, but not in others, the macroscopic deformation could be accounted for in terms of geometric changes in the stacked crystalline and amorphous layers which constitute the long period. In these previous studies the samples were held at constant strain, and an unknown amount of stress relaxation occurred before and during X-ray analysis. In the present work the axial stress was determined, in addition to the strain, and this proved to be of value in terms of the information obtainable about the role of the long period structure in deformation of the fibre.

Deformation mechanisms which have been known to produce or contribute to large strains in oriented crystalline polymers at room temperature are (a) extension of the intercrystalline amorphous polymer, (b) interlamellar slip, (c) intermolecular slip, and (d) interfibrillar slip. In axial compressions and extensions mechanism (a) is, in LDPE, a major process [8] and, in some linear polymers, even the sole process [6], while mechanism (b) may be of small but significant importance in LDPE [8]. With uniaxial stress applied at an angle to the chain axes, mechanism (c) is the primary mode of deformation at normal strain rates for plastic flow in linear polyethylene in compression [9]; this is also true for polypropylene [10] and linear polyethylene [11] in tension, although in these cases contributions due to mechanism (d) were detected.

In this paper new data on the axial deformation of oriented LDPE will be interpreted in the light of established ideas of morphology and deformation mechanisms in fibre structures, and will be linked with results of earlier studies on this subject in LDPE and other polymers. The conclusions may be applicable to a more general range of crystalline polymer fibres.

2. Experimental

2.1. Preparation of samples

The polymer was a branch-containing polyethylene of low density, ICI Alkathene WJG 11, which was obtained as granules. Compression moulded sheets were prepared and then oriented by uniaxial drawing at a room temperature, 20 ± 3° C. This drawn material retracted considerably on unloading in the tensometer and the axial draw ratio was × 3.2 after several months of stabilization at room temperature. Tensile specimens were cut from the drawn sheets with their long axes at 0° to the orientation direction. The gauge dimensions of the specimens were approximately 2.0 mm width, 0.5 mm thickness and 40 mm length. A 0.2 mm grid of ink dots was impressed onto the specimens to facilitate measurements of strain.

2.2. Methods of straining and strain measurements

Each tensile specimen was clamped at its ends in movable grips and mounted in a small frame. The frame was placed on the bed of the X-ray camera. allowing X-ray photographs to be taken during deformation. A load was applied, and the initial strain noted (the specimen was held at its initial strain for about 1 min in order to obtain a strain measurement; the constraint was then removed). Strain was subsequently observed at intervals for the duration of the experiment. Several samples were studied, in each case using a different static load. In a further experiment a sample was subjected to additional static loads, which were applied after suitable time intervals. In those samples which were deliberately unloaded, the strain retained immediately after removal of the load was measured.

Axial strain measurements were made by means of a travelling microscope focussed on a grid of ink dots on the surface of the specimen, while width and thickness strains were measured by micrometer. Straining occurred uniformly along the gauge length, but strains were measured in the region of the sample that was exposed to the X-ray beam. All deformations were carried out at the same temperature as in the initial drawing, 20 ± 3° C.

2.3. X-ray methods

All X-ray photographs were taken using pinhole collimation with a beam diameter at the sample

of 0.3 mm. Except where noted, the beam direction was parallel to the width and perpendicular to the fibre axis of the sample. Diffraction patterns at wide and low amgles could be recorded simultaneously in the same camera; 40 kV nickel filtered copper radiation was used. The specimen–film distance was 330 mm in low angle and 40 mm in wide-angle diffraction; exposure times were about 15 and 3 h respectively.

Densitometer scans were taken parallel to the meridian in the low-angle photographs and, from the intensity peaks, fibre long periods were calculated using Braggs law. (The use of Braggs law may not be strictly justified for the absolute determination of long spacings but we will be concerned only with relative changes, so that errors arising from this procedure will be negligible.)

3. Results

3.1. Initial oriented material

X-ray photographs taken from the initial oriented material are shown in Fig. 4a. Diffraction at low angles is essentially a pair of meridional streaks and there is no continuous scattering due to voids. The long period, as calculated from the vertical separation of the layer lines, was 109 Å. The (2 0 0) and (1 1 0) arcs in wide-angle diffraction indicate that, for the crystalline component, the molecules were mainly aligned along the draw axis. A wide-angle photograph (not shown) taken with the beam parallel to the fibre axis showed that the *a*-axes (2 0 0 diffraction) and *b*-axes (0 2 0 diffraction) were uniformly distributed about the orientation axis. The material was fairly transparent in appearance and there was no stress-whitening.

3.2. Elastic response

On the time scale of interest in this work the tensile behaviour of the material was almost an instantaneous elasticity, i.e. creep was very small or not observed, for axial stress up to 13 MN m^{-2} (strains up to 7%). Data for two of the samples studied in this range of stress are quoted: the initial strains were 5% and 7%, and the loading times 211 and 245 h respectively. For the sample at 5% strain no creep was detected, while the sample at 7% initial strain had a final strain of 8%. In both of these samples ϵ_d, the strain in the fibre long period, was constant during loading at values in each case similar to ϵ, the macroscopic strain. When these samples were unloaded the sample lengths and the fibre long periods practically completely recovered to their former values within the time required to make measurements (incomplete recovery in the long period was about 1%, i.e. just detectable, in the sample at the higher strain). Data for this elasticity is plotted in Figs. 2 and 5, using symbols with the subscript "e", and is consistent with other data in those figures derived

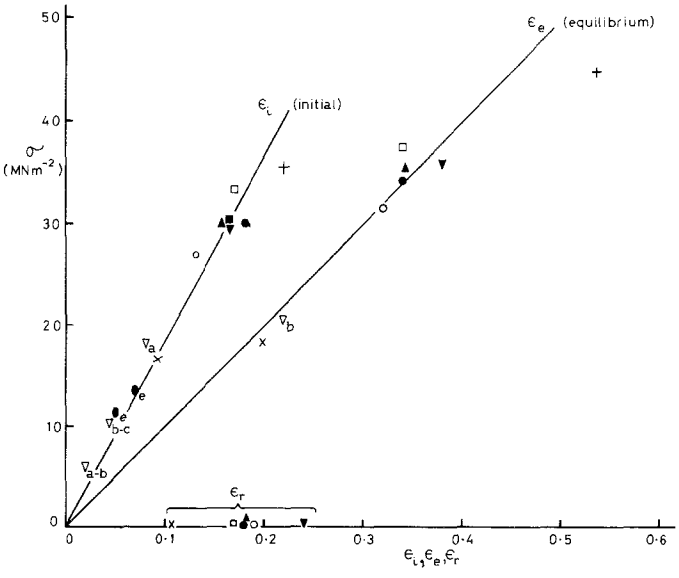

Figure 2 Initial elastic strain (ϵ_i), equilibrium creep strain (ϵ_e), plotted against true stress (σ). Samples having strains ϵ_e which were unloaded (Section 3.3.3) retracted instantaneously to strains ϵ_r, which are plotted on the $\sigma = 0$ axis. $\bullet_e$ = samples exhibiting low elasticity (Section 3.2) ∇ = sample with stepped loading (Section 3.3.2). Other symbols = creep at constant load (Section 3.3.1).

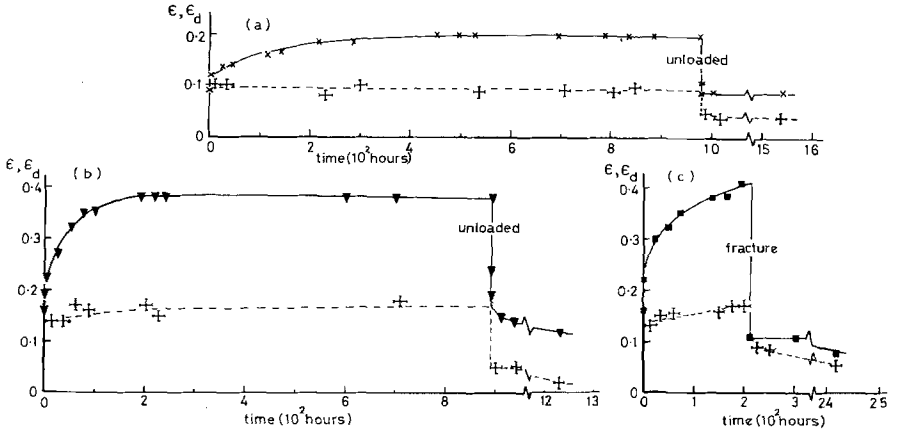

Figure 3 Time dependence of macroscopic strain ϵ (full lines) and long period strain ϵ_d (broken lines) for samples subjected to nominal stresses. (a) 15.4 MN m^{-2}; (b) 25.8 MN m^{-2}; (c) 25.9 MN m^{-2}.

from the experiments of Section 3.3.

For stresses of 16 MN m^{-2} or greater (initial strain $\geqslant$ 8%) the material exhibited creep (Section 3.3). However, in a test for elastic behaviour in this range, several samples were subjected to stresses up to about 40 MN m^{-2} (strains up to 22%) and the loads were removed within 1 min. These samples immediately recovered their initial dimensions and the structure, as subsequently determined by X-ray diffraction, was unchanged by the stress cycle, the main feature being that the long period was the same as for the initial material.

3.3. Tensile creep and recovery

3.3.1. Creep at constant load

In these experiments strain was measured initially (ϵ_i) and at intervals as elongation took place at constant load. Eight samples were studied in a range of nominal stresses (σ_0) from 15.4 to 28.9 MN m^{-2} (initial strains 9% to 20%). Even at the highest creep strains, some 50%, there was no observable stress-whitening and the increase of sample volume was only 3 ± 2%. Straining was therefore reckoned to occur essentially at constant volume and true stresses (σ) were calculated using the formula $\sigma = \sigma_0 (1 + \epsilon)$. Initial strain is plotted against true stress in Fig. 2, and from the linearity the initial modulus is 182 MN m^{-2}.

X-ray data were obtained at intervals during creep, the major change, and the principal quantity of interest, being the strain in the fibre long period. The quantities ϵ and ϵ_d are plotted against time in Fig. 3 for three of the samples. Figs. 3a and b are for nominal stresses 15.4 and 25.8 MN m^{-2} respectively. A principal feature of the macroscopic behaviour is that a quasi-equilibrium strain (ϵ_e) was reached. The near-constancy of the equilibrium strain at long times as shown in Fig. 3a and b is representative of all the samples which did not rupture. Equilibrium strain is plotted against true stress in Fig. 2 and a direct proportionality is indicated, with equilibrium creep modulus of 98 MN m^{-2}. X-ray patterns for the sample of Fig. 3b taken during creep at strain $\epsilon \approx 35\%$ are shown in Fig. 4b. The small-angle pattern remains basically a pair of meridional streaks, and the wide-angle pattern indicates that molecular orientation is slightly improved in comparison with the initial material. Fig. 3c shows data for a sample with nominal stress 25.9 MN m^{-2} which ruptured. (Four of the samples ruptured, in one case after an equilibrium strain had been reached, and the rupture stresses were 44.3, 37.2, 36.3 and 38.0 MN m^{-2}.)

Changes in ϵ_d were small during creep, although at the higher stresses, as represented by Fig. 3b and c a significant increase is evident. Owing to exposure times for diffraction at small angles, ϵ_d values could not be taken with the sample at constant strain. In particular, long periods corresponding to the initial elastic strain could not be obtained. However, in Fig. 5 we compare the initial sample strain (ϵ_i) with the initial value of the long period obtained during creep (ϵ_{di}) and it is seen that the experimental points indicate equality of ϵ_{di} and ϵ_i.

The value of ϵ_d did not increase in any of the samples after the equilibrium strain had been reached; equilibrium values of ϵ_d are denoted ϵ_{de}. Fig. 6 shows that ϵ_{de} is directly proportional to

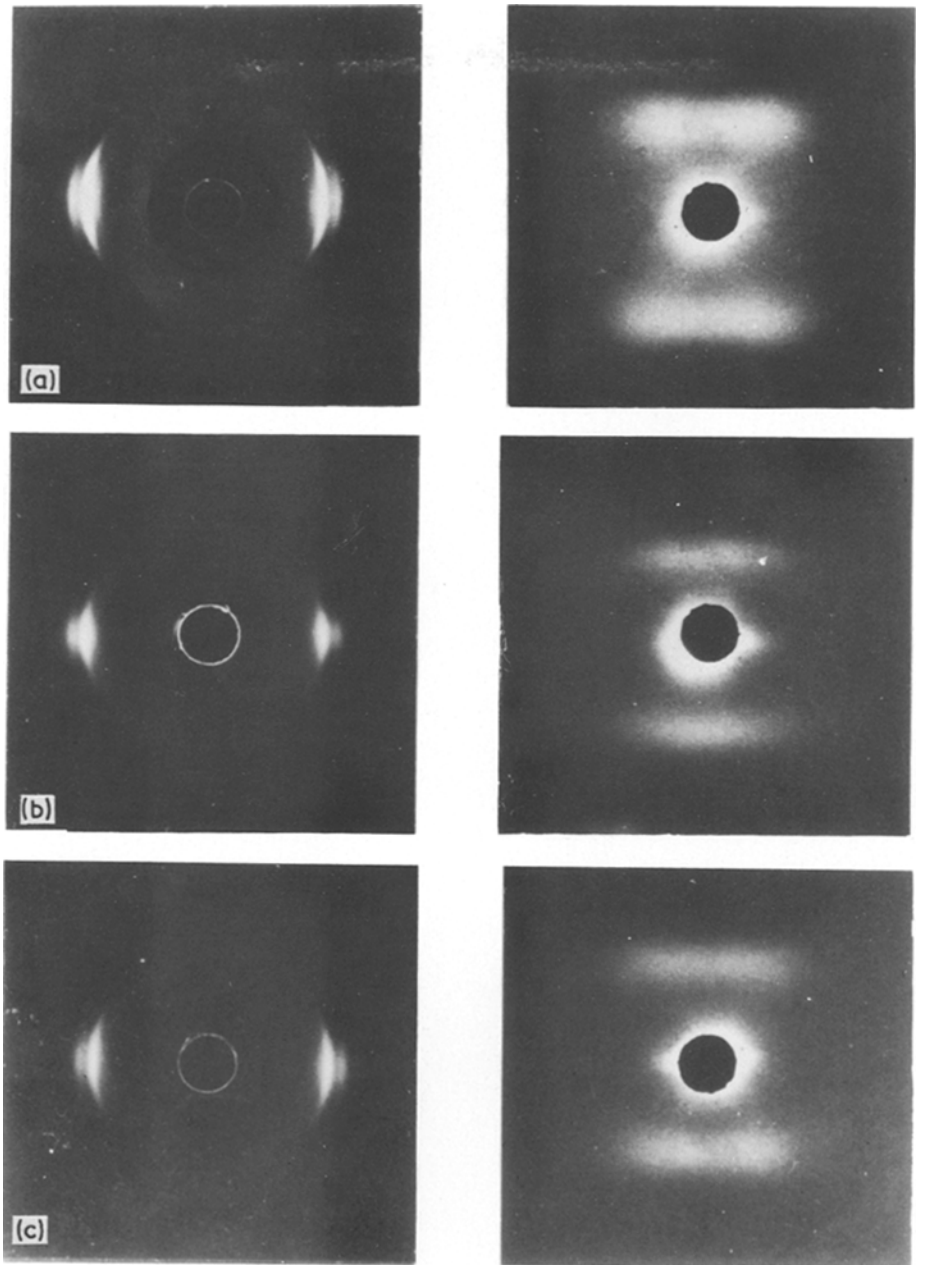

Figure 4 Low- and wide-angle photographs for (a) initial material, draw ratio = 3.2, (b) sample of Fig. 3b at creep strain ~ 35%, (c) sample of Fig. 3b after unloading. The initial draw direction and the stress axis are vertical in all pictures.

stress, the modulus σ/ϵ_{de} being $188\,MN\,m^{-2}$.

Rates of creep for the samples which reached equilibrium are compared by normalizing the creep strain $(\epsilon_e - \epsilon_i)$ to a common ordinate. This is done in Fig. 7 by plotting relative strain, $[\epsilon(t) - \epsilon_i]/(\epsilon_e - \epsilon_i)$, the fraction of the creep strain reached at a time t, against log t. Relative strains fit reasonably well to a common creep curve, and the time to reach 63% of $(\epsilon_e - \epsilon_i)$ is 45 ± 10 h. However, for time in the range shown in Fig. 7 the data are consistent with the relation (full line) $f(t) = (1 - 0.74\,e^{-t/\tau})$ where $\tau = 68$ h, so that the retardation time for the main part of the creep process is of this order; relaxation at creep times over the range 0 to 10 h, which was not studied in detail, must be somewhat faster. Fig. 7 also includes data for a sample with previous creep history (Section 3.3.2).

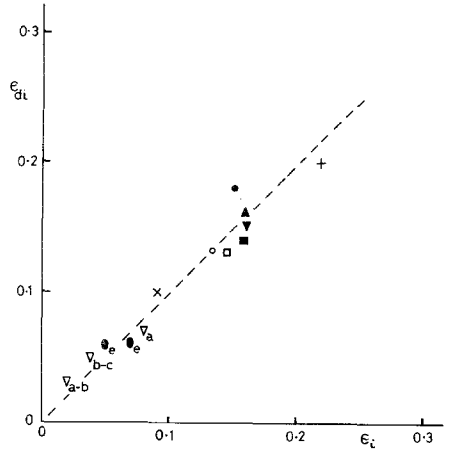

Figure 5 Comparison of initial elastic strain (ϵ_i) with initial long period strain (ϵ_{di}). The broken line indicates $\epsilon_i = \epsilon_{di}$ Symbols as for Fig. 2.

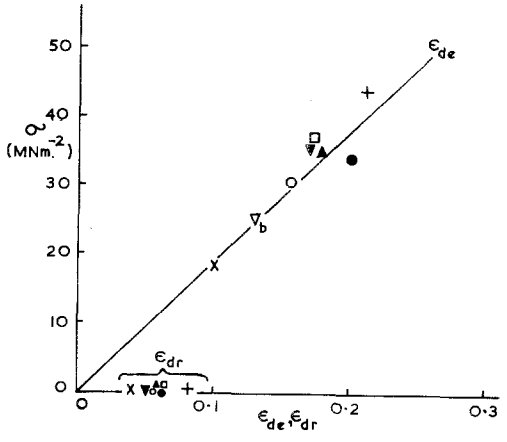

Figure 6 Equilibrium long period strain (ϵ_{de}) plotted against true stress (σ). Samples which were unloaded retained long period strains ϵ_{dr}, which are plotted on the $\sigma = 0$ axes. Symbols as for Fig. 2.

3.3.2. Creep with stepped loading

Fig. 8 shows the tensile response of a sample to which additional loads were applied at times 75 and 295 h after initial loading. Nominal stresses in the regions a, b, c were 16.9, 20.7 and 28.6 MN m^{-2} respectively. Data from Fig. 8 are included in Figs. 2 and 5 to 7. The experimental points are labelled a, b, a–b and b–c; a, b, refer to quantities in the regions a and b, while a–b and b–c refer to changes in the quantities in passing from one region to another.

The three load applications produced similar changes in ϵ and ϵ_d (Fig. 5), of magnitude in accordance with the results of Section 3.2 and 3.3.1 ($\sigma/\epsilon_i = 182$ MN m^{-2}, Fig. 2). Also, for region b, the creep curve (Fig. 7), equilibrium creep modulus (Fig. 2) and equilibrium long period strain (Fig. 6) are consistent with the results for creep at constant load.

3.3.3. Recovery

The creep specimens of Section 3.3.1 which had reached equilibrium were unloaded. The strains retained by the samples immediately after removal of load are denoted ϵ_r and are plotted along the $\sigma = 0$ axis in Fig. 2 (one sample at equilibrium, which ruptured, is excluded). A further recovery of the samples occurred, mainly within a few hours. The time dependence of the overall strain recovery was not studied in detail, but, as is evident from Fig. 3, it was not similar to the time

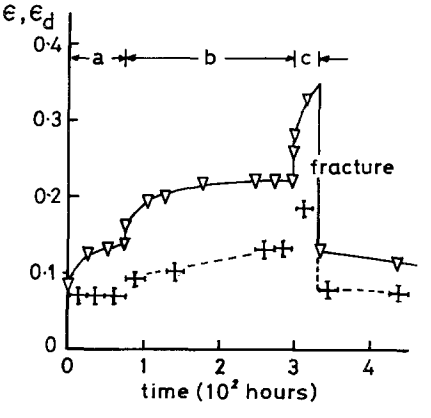

Figure 8 Time dependence of macroscopic strain ϵ (full line), and long period strain ϵ_d (broken line) for a sample subjected to nominal stress. (a) 16.9 MN m^{-2}, (b) 20.7 MN m^{-2}, (c) 28.6 MN m^{-2}.

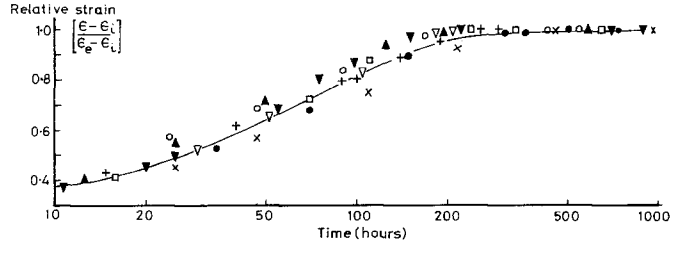

Figure 7 Relative strain plotted against time. The experimental points are shown in relation to the curve $f(t) = (1 - 0.74\, e^{-t/\tau})$, where $\tau = 68$ h. Symbols as for Fig. 2.

dependence of the tensile creep described in Section 3.3.1: there was little further recovery at times more than 10 h after unloading, and recovery was incomplete in all cases.

After unloading the fibre long periods did not completely retract to their initial values, a result which is in contrast to the experiments of Section 3.2 in which samples were loaded for short times. The first measured values of ϵ_d following unloading are denoted ϵ_{dr}, and are plotted along the $\sigma = 0$ axis in Fig. 6. Further recovery of the ϵ_d values was small or zero on a time scale of 100 h after unloading.

4. Discussion and interpretation

4.1. Elastic response

The nearly Hookean elasticity currently observed for strains up to 7% and loading times of some 250 h is in keeping with the results of Darlington *et al.* [12], who found that in oriented LDPE of draw ratio 3.8 (tensile modulus $E_0 \simeq 420\,\mathrm{MN\,m^{-2}}$) tensile creep was almost negligibly small for times up to 1000 sec at 1% strain and also, in a 100 sec isochronous creep test, for strains up to 4%. In the present experiments this relaxation occurred effectively instantaneously on our time scale, changes in ϵ and ϵ_d were similar (Fig. 5), and the only significant change in the X-ray patterns resulting from the sample strain was that the vertical separation of the low-angle maxima decreased, while remaining as broad layer-line streaks. There was, therefore, no appreciable rotation of the crystal surfaces, and so we can identify the main deformation process to be that the crystal cores undergo a reversible increase in separation which fully accounts for the increase in sample length. Here, we note that in the axial extension of various oriented polymers the crystal lattice has been found to be practically rigid, [6, 13, 14], by far the greater part of the long period increase being due to stretching of the rubbery amorphous polymer which resides between the crystals.

On the isolated evidence of Fig. 5 a possible explanation for the result $\epsilon = \epsilon_d$ is that the crystalline and amorphous layers merely strain uniformly with respect to some material in which they may be embedded. However, it is shown in Section 4.2 that the layers experience the full applied stress. From these facts we conclude that the periodic arrays which produce the small-angle diffraction are the controlling elements in the elasticity, and make up the bulk of the sample: if there were a significant fraction of some other phase present then that phase does not contribute to the diffraction at low angles, and it must also have tensile properties which are similar to the other sample material. In view of the peculiar make-up of the long period structure, the possibility of any such "third-phase" can be practically excluded, except in small amount (at higher temperatures there may be partial melting of the crystals, which could produce amorphous polymer which would surround the stacks [15]).

Equality of ϵ and ϵ_d as observed in the above elasticity has been noted in certain other instances in which oriented polymers were stressed parallel to the draw axis at room temperature, as follows:

(a) compressive strains up to 30% in LDPE [7, 8], and compressive strains up to 20% in linear polyethylene [7];

(b) tensile stresses up to 15% in linear polyethylene [6, 7], and various other linear polymers such as polypropylene, polyethylene terephthalate, and polyvinyl alcohol [6].

The loading times in experiments a and b, were not stated, but practically no irreversible changes in the macroscopic dimensions or in the microstructure occurred in the time needed to obtain X-ray data, and the deformations were attributed wholly or mainly to elastic translations of the crystals with only small, if any, interlamellar slip or other deformation mechanisms.

In contrast with (a) and (b) above it has been observed [7, 8] that for LDPE in tension $\epsilon_d \simeq 0.7\epsilon$ for ϵ up to 20% and there was considerable permanent set [8]. It will be shown in Section 4.2 that this result is due to the occurrence of creep in LDPE in tension, which apparently has little or no effect on the geometry of the stacked crystalline and amorphous layers and may, in fact, originate outside its fibrils. The present work thus clarifies the situation in that we can recognize that it is normally only in extensions or compressions of polymer fibres where creep does not occur, and hence where the deformation is reversible, that equality of ϵ and ϵ_d is to be expected (an anomalous case seems to be that of oriented nylon in tension, where it has been observed [4, 5, 7] that $\epsilon < \epsilon_d$, a result attributed to non-uniform deformation of the polymer volume [4].

4.2. Creep at constant load

Tensile creep in cold-drawn LDPE at times up to

10^3 sec has been widely studied by Darlington *et al.* [12, 19] who found that little creep occurred at all angles to the orientation axis, creep being particularly small when stress was applied parallel to the chain direction [12]. With uniaxial tension applied at 45° to the chain axes, creep was associated with easy shear parallel to the chain axes; other creep mechanisms were believed to become important at angles near 0°, and also near 90° where increased non-linearity was observed [19]. Creep at long times in oriented LDPE, as reported here, has apparently not been previously studied.

Fibre long periods corresponding to the initially-loaded samples were not obtainable, due to X-ray exposure times. However, it will be assumed that the first values of ϵ_d measured during creep, denoted ϵ_{di}, correspond closely to the initial strains in the long period. The equality of ϵ_i and ϵ_{di} (Fig. 5) suggests that this approximation is valid, and that the arguments of Section 4.1 for small elastic elongations are applicable. It is therefore concluded, as before, that the initial elastic extensions are determined by the axial elastic properties of the crystalline and amorphous layers which largely make up the structure: this is now seen to hold for initial strains up to 20%.

In the present experiments, as in the work of Darlington *et al.* [12], changes in the form of the X-ray diffraction occurring as a result of creep were rather small. A comparison of the diffraction photographs of Fig. 4a (initial material) and b (during creep) shows that in the strained sample there is a slight shift of intensity at low angles towards the meridian, indicating that the diffracting elements have rotated by a small amount, but in the opposite sense to that which would occur in interlamellar slip in tension with accompanying rotation of the lamellae [15]. Interlamellar slip is, therefore, not the predominant deformation mode in creep. If shear takes place parallel to the molecules, whether by chain or interfibrillar slip, the molecular axes converge towards the tensile axis, as observed. However, our stress system was chosen to favour an analysis of the long period strains, and the X-ray data does not directly allow us to distinguish between these two mechanisms because the molecular axes (c) and the lamellar normals (n_L) are at all stages distributed about the tensile axis (in inter-fibrillar slip the angle $\widehat{cn}_L$ would be unaltered, whereas in homogeneous molecular slip this angle would change [9]).

Since increases in ϵ_d during creep were small in relation to the sample strain, the creep cannot be accounted for in terms of an affine elongation of the crystalline and amorphous layers, as was the case in instantaneous elasticity. We therefore enquire into the origin and nature of a relaxation mechanism which produces that part of ϵ which cannot be accounted for by ϵ_d. In several studies (e.g. [3, 6, 9]) it has been suggested that a fibre structure may deform under axial stress by longitudinal displacement of the fibrils past each other, this process being opposed by interfibrillar tie molecules and molecular bonding. A relative displacement of the fibrils, which incorporate the stacked crystals, would account for the fact that $\epsilon > \epsilon_d$ if such a process made an appreciable contribution to the total deformation, (in the extreme case of undeformable fibrils the sample would elongate under applied stress as a result of fibrils sliding along one another, and the period of alternation inside the fibrils would not change). Figs. 2 and 5, which relate to initial elastic deformations, suggest that the tensile modulus of the fibrils may be the same as that of the macroscopic sample, $182\,MN\,m^{-2}$. If the long period strain depends only on stress then in a creep test at constant stress there would again be no increase in ϵ_d. However, we presently have creep at constant nominal stress, essentially at constant volume, and there is thus a stress increase due to decrease of sample cross-section. Hence if the fibrils experience the full applied stress during creep, as they appear to do in the initial elasticity, then ϵ_d should increase in accordance with a modulus of some $182\,MN\,m^{-2}$. Fig. 6 shows that this is the case: the indicated modulus of the fibrils with the samples at equilibrium creep strain is $\sigma/\epsilon_{de} = 188\,MN\,m^{-2}$ which is within the experimental error equal to the initial modulus of the bulk sample. These results show that during initial elasticity and creep the long period structure is in equilibrium with the applied stress, i.e. there is no detectable degree of parallel connection with any surrounding interfibrillar material. It has frequently been a problem in oriented polymers to decide how the different structural components of the multiphase material respond to stress, i.e. whether the conditions are equal stress (wholly series connection), equal strain (wholly parallel connection), or some situation intermediate between the two. Takayanagi *et al.* have shown

[2] that the crystalline and amorphous regions in linear polyethylene are arranged mainly in series along the orientation axis even though the material is fibrillar. The present results are not concerned with the stress distribution within the fibrils, but apparently the fibrils themselves are in series connection even in a large-scale creep deformation, and strain by an amount unrelated to the total strain in the sample, which is partly produced by other relaxation mechanisms.

Leadermann has found [16] that uniaxial tensile creep in nylon 66, silk, and rayon, all oriented crystalline fibres, is non-linear under many experimental conditions. This lack of linearity was attributed to stress-induced recrystallization which made the fibres stiffer, and hence the material was structurally different at the end of the loading experiment from what it was at the beginning. In contrast to this, the present results suggest that in creep in oriented LDPE the crystalline and amorphous stacks, and the fibrils, are permanent features of the fibre structure, and the creep process is, therefore, likely to involve simpler mechanical deformations in the existing structure. This argument is reinforced by the fact that the samples have an equilibrium strain which is evidently nearly constant for long times (Fig. 3), and so the material appears to attain a state of high elasticity characteristic of equilibrium in a permanent molecular network. Bond rupture, or the detachment of chains or even larger fragments from the periphery of crystallites, which are processes which have been suggested in other cases of slow creep in polymers, would be unlikely to produce an equilibrium strain.

If changes in the basic structure of the material are small, linear creep may be expected. Fig. 7 shows that an exponential relative strain curve is an approximate representation of all the creep curves for creep times greater than about 10 h, so that creep may occur largely by a unimolecular process. Creep as slow as this is not likely to be produced by the relaxing of single network strands, but may be due to a co-operative process involving groups of molecules which extend through larger regions of the relaxing network. That very slow creep would result from such a process has been shown theoretically by Bueche (see [17]). According to Point (see [8]) the interfibrillar material in LDPE contains extended-chain crystals: these crystals could act as the network junctions or cross-links which couple the strands. Since the fibrils are in series connection, the interfibrillar material may also be subjected to the full applied stress, i.e. the fibrils homogenize the stress field, as has been noted by Peterlin [18].

Intermolecular slip must be held as the other distinct possibility for the creep process, being due to shear on those chains not fully aligned in the draw direction. This process would be hindered if the chains traverse several crystals. A difficulty with this mechanism, in which the crystals themsleves are sheared, is to explain how it could occur while maintaining the direct proportionality between the long period strain and stress (Fig. 6); it is also unclear how chain slip would produce a steady state compliance independent of stress Fig. 2).

A further difficulty in explaining the present results on the chain slip model is that large rotations of the crystal surfaces are expected, yet changes in the low-angle pattern are small: following Shinozaki and Groves [10] a planar shearing of the molecules would rotate the crystal surfaces, and hence the small angle maximum of a given stack of lamellar crystals, through an angle $\tan^{-1}\alpha$, where α is the glide strain given by:

$$\alpha = \frac{1}{\sin\theta_0}\left\{\sqrt{\left[\left(\frac{l_1}{l_0}\right)^2 - \sin^2\theta_0\right]} - \cos\theta_0\right\}. \quad (1)$$

Here, l_0 and l_1 are the lengths before and after extension, and θ_0 is the initial angle between the chain and tensile axes for the particular stack considered. Putting $\theta_0 = 5^\circ$ (an intermediate value, Fig. 4a) we find that a creep strain due to chain slip of, say 15% would cause a rotation of the crystal surfaces by an angle $\tan^{-1}\alpha \simeq 60^\circ$. The counteracting effect of an overall rotation of the molecular axes would be negligible by comparison, and the rotations would clearly be greater in those stacks having smaller values of θ_0. The similarity of the small angle patterns of Fig. 4a (initial) and b (during creep) suggests that rotations of this magnitude do not occur. Also, as there is permanent set due to irreversibility of the creep mechanism, the rotations just discussed would not be fully reversible, and yet the small angle patterns were nearly the same after unloading (Fig. 4c) as initially.

An approximate model for the tensile behaviour is shown in Fig. 9. Instantaneous response of the material and of the long period is indicated by a spring of modulus $E_0 = 185\,\mathrm{MN\,m^{-2}}$, while viscoelasticity is represented

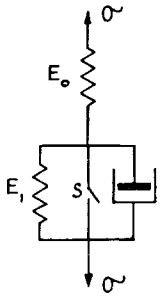

Figure 9 Approximate mechanical model for tensile creep in oriented LDPE. Spring E_0 (185 MN m^{-2}) represents instantaneous elasticity. Spring E_1 (208 MN m^{-2}) and the dashpot represent creep. "Switch" S opens at stress $\sigma \simeq$ 13 MN m^{-2}.

by a spring E_1 in parallel with a dashpot. The parallel element is effectively rigid for small strains, so a switch S is included which breaks at tensile stress $\simeq 13$ MN m^{-2}, possibly indicating a critical shear stress for the creep mechanism. When E_1 reaches equilibrium with the stress, the strain ϵ_e is attained and, from Fig. 2, the equilibrium tensile creep modulus E_∞ is 98 MN m^{-2}. Using the series spring relation,

$$\frac{1}{E_\infty} = \frac{1}{E_0} + \frac{1}{E_1}$$

we obtain $E_1 = 208$ MN m^{-2}.

The deformation mechanism in LDPE in axial tension which produces the result $\epsilon > \epsilon_d$ as observed here and elsewhere [7, 8] appears to have been of little significance in linear polyethylene or other linear polymers which have been similarly studied. Resolved shear stresses for chain slip in linear polymers would be smaller, owing to the higher degree of molecular orientation. Alternatively, Peterlin has suggested [18] that interfibrillar slip in linear polymers would be more difficult than in LDPE, due to the substantial difference in draw ratio, which yields proportionately longer fibrils: the longer the fibril, the greater the surface to cross-section ratio, and hence the resistance to shear displacement. However, the final stages in drawing of fibres, and hence the fact that long periods are largely independent of draw ratio λ in linear polyethylene and polypropylene for $\lambda \geqslant 3$, is proposed to be due to interfibrillar slip [3]. If controlled by a molecular process as stiff as that seen here in LDPE, interfibrillar slip would not be expected to produce plastic flow (easy shear) at normal strain rates, and in fact in linear polyethylene and polypropylene this occurs predominantly by chain clip [9. 10, 11]. Creep is probably small in oriented LDPE in axial compression, since $\epsilon \simeq \epsilon_d$ in this case [7, 8], and strains are nearly fully recoverable.

4.3. Creep with stepped loading

Here, arbitrary load increases which were applied after periods of creep produced abrupt changes in ϵ and ϵ_d which are as expected from the results of creep experiments with constant load. There was, therefore. no observable strain hardening either of the sample or of the internal crystalline/amorphous periodicity, even after creep. Since there was no strain hardening for the initial strains in the constant load experiments, this result is to be expected if the instantaneous elasticity of the fibrils is independent of the creep mechanism.

The facts that in region b (Fig. 8) the equilibrium strain, and also the time dependence of relative strain, fit the curves of Figs. 2 and 7, indicates that the deformation at a given time depends upon the previous loading history, and that the total deformation is the summation of the deformations caused by the separate incremental loads.

4.4. Recovery

In view of the results for instantaneous tensile response, recovery of strain in the crystalline and amorphous layers may be expected to account for the sudden decrease in sample strain which occurs when the internal compressive forces are released at the time of unloading. We may test for this by comparing the relative compression of the fibre long period with the relative compression of the sample: for an affine retraction of the long period with respect to the sample length it is required that

$$\frac{\epsilon_r - \epsilon_e}{1 + \epsilon_e} = \frac{\epsilon_{dr} - \epsilon_{de}}{1 + \epsilon_{de}} \qquad (2)$$

where the retained long period strain ϵ_{dr} as measured is small, and practically constant, and is reckoned to be the value of ϵ_d immediately after unloading. The above relationship is examined in Fig. 10, where it is seen that the recovery of the sample is comparable with, although slightly more than, the recovery of the long spacing.

In a creep test at constant stress the strain immediately recovered when the load is removed is normally the same as the initial strain. In the present case if the fibrils do not creep (Section

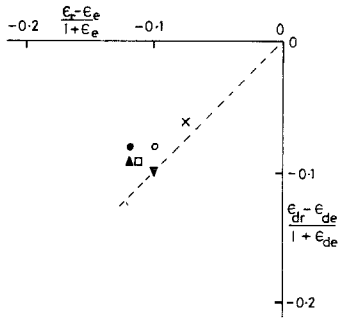

Figure 10 Relative macroscopic retraction $(\epsilon_r - \epsilon_e)/(1 + \epsilon_e)$ plotted against relative retraction of the long period for samples unloaded after reaching equilibrium in creep at constant load. The broken line indicates equality.

4.2), then when the sample strain is ϵ_e, the instantaneous tensile strain component will be greater than its initial value by the factor $(1 + \epsilon_e)/(1 + \epsilon_i)$. As the long periods retain a strain ϵ_{dr}, we expect the quantity

$$\Delta\epsilon = \left(\frac{1+\epsilon_e}{1+\epsilon_i}\right)\epsilon_i - (\epsilon_e - \epsilon_r) \qquad (3)$$

to be positive, and of magnitude similar to ϵ_{dr}, if the sample and the fibrils recover by the same proportions. Table I shows that $\Delta\epsilon$ is indeed positive and comparable with, but in most cases a little smaller than ϵ_{dr}.

TABLE I Comparison of the retained long period strains (ϵ_{dr}) with the unrecovered "instantaneous" strains in the samples ($\Delta\epsilon$) as evaluated using Equation 3.

Sample (symbols as for Fig. 2)	$\Delta\epsilon$	ϵ_{dr}
×	0.01	0.04
○	0.02	0.06
●	0.04	0.06
▲	0.03	0.06
□	0.03	0.06
▼	0.06	0.05

The above discussions show that the retraction of the crystalline and amorphous layers accounts for nearly all of the instantaneous retraction of the sample.

Following the rapid recovery at unloading the samples contracted by a further amount, this mainly occurring within a few hours. In ideal viscoelasticity the time dependence of strain recovery is the same as that of stretching, but in real polymers this is commonly not the case, because the stress-biased diffusion of segments is not identical with free diffusion. The occurrence of permanent set in the long period is surprising if the fibrils do not creep. However, a permanent set in LDPE has been observed [8] even in the absence of creep.

5. Conclusions

The main conclusions of this work are as follows: Uniaxially oriented LDPE was subjected to static axial loading at room temperature. At all creep times and stresses the strain in the fibre long period was directly proportional to the applied stress; the tensile modulus for this microstructural process was equal to the initial tensile modulus of the material. Therefore, the stacks of crystalline and amorphous layers, and the fibrils into which they are assumed to be incorporated, were in fully series connection but did not observably contribute to creep except insofar as could be accounted for by the stress increases involved. Longitudinal deformation of the fibrils did, however, control the instantaneous elasticity in tension and recovery. Interlamellar slip appeared not to be of importance. Except for short times of loading retraction of the material in free recovery was incomplete, and the time dependence of the partial recovery was not the same as in tensile creep; there was also a small permanent set in the long period. Creep was almost negligibly small on our time scale for tensile stresses less than about 13 MN m^{-2}. Interfibrillar slip appeared as a likely creep mechanism, but chain slip is also a possibility; in either case, a co-operative process would be required.

References

1. R. HOSEMANN, *J. Appl. Phys.* **34** (1963) 25.
2. M. TAKAYANAGI, K. IMADA and T. KAJIYAMA, *J. Polymer Sci.* **C15** (1966) 263.
3. A. PETERLIN, *J. Mater. Sci.* **6** (1971) 490.
4. D. R. BERESFORD and H. BEVAN, *Polymer* **5** (1964) 247.
5. A. I. SLUTSKER, T. P. SANPHIROVA, A. A. YASTREBINSKII and V. S. KUKSENKO, *J. Polymer Sci.* **C16** (1968) 4093.
6. S. N. ZHURKOV, A. E. SLUTSKER and A. A. YASTREBINSKII, *Sov. Phys. Solid State* **6** (1965) 2881.
7. K. ISHIKAWA, Z. MIYASAKA, M. MAEDA and M. YAMADA, *J. Polymer Sci.* **A2** (1969) 1259.
8. A. KELLER and D. P. POPE, *J. Mater. Sci.* **6** (1971) 453.
9. R. J. YOUNG, P. B. BOWDEN, J. M. RITCHIE and J. G. RIDER, *ibid* **8** (1973) 23.
10. D. M. SHINOZAKI and G. W. GROVES, *ibid* **8** (1973) 1012.
11. T. HINTON, J. G. RIDER and L. A. SIMPSON, *ibid* **9** (1974) 1331.

12. M. W. DARLINGTON, B. H. MCCONKEY and D. W. SAUNDERS, *ibid* **6** (1971) 1447.
13. W. J. DULMAGE and L. E. CONTOIS, *J. Polymer Sci.* **28** (1958) 275.
14. S. NEWMAN and R. L. MILLER, *ibid* **60** (1972) 14.
15. A. COWKING, J. G. RIDER, I. L. HAY and A. KELLER, *J. Mater. Sci.* **3** (1968) 646.
16. H. LEADERMAN, "Elastic and Creep Properties of Filamentous Materials" (The Textile Foundation, Washington D.C., 1943).
17. T. ALFREY, "Mechanical Behaviour of High Polymers" (Interscience, New York, 1948).
18. A. PETERLIN, *Macromol. Chem.* **8** (1972) 277.
19. M. W. DARLINGTGN and D. W. SAUNDERS, *J. Phys.* **D3** (1970) 535.

Received 31 January and accepted 26 March 1975.